The American Journal of Human Genetics, Volume *99*

Supplemental Data

Loss-of-Function Mutations in *ELMO2* Cause Intraosseous Vascular Malformation by Impeding RAC1 Signaling

Arda Cetinkaya, Jingwei Rachel Xiong, İbrahim Vargel, Kemal Kösemehmetoğlu, Halil İbrahim Canter, Ömer Faruk Gerdan, Nicola Longo, Ahmad Alzahrani, Mireia Perez Camps, Ekim Zihni Taskiran, Simone Laupheimer, Lorenzo D. Botto, Eeswari Paramalingam, Zeliha Gormez, Elif Uz, Bayram Yuksel, Şevket Ruacan, Mahmut Şamil Sağıroğlu, Tokiharu Takahashi, Bruno Reversade, and Nurten Ayse Akarsu

Supplemental Figures

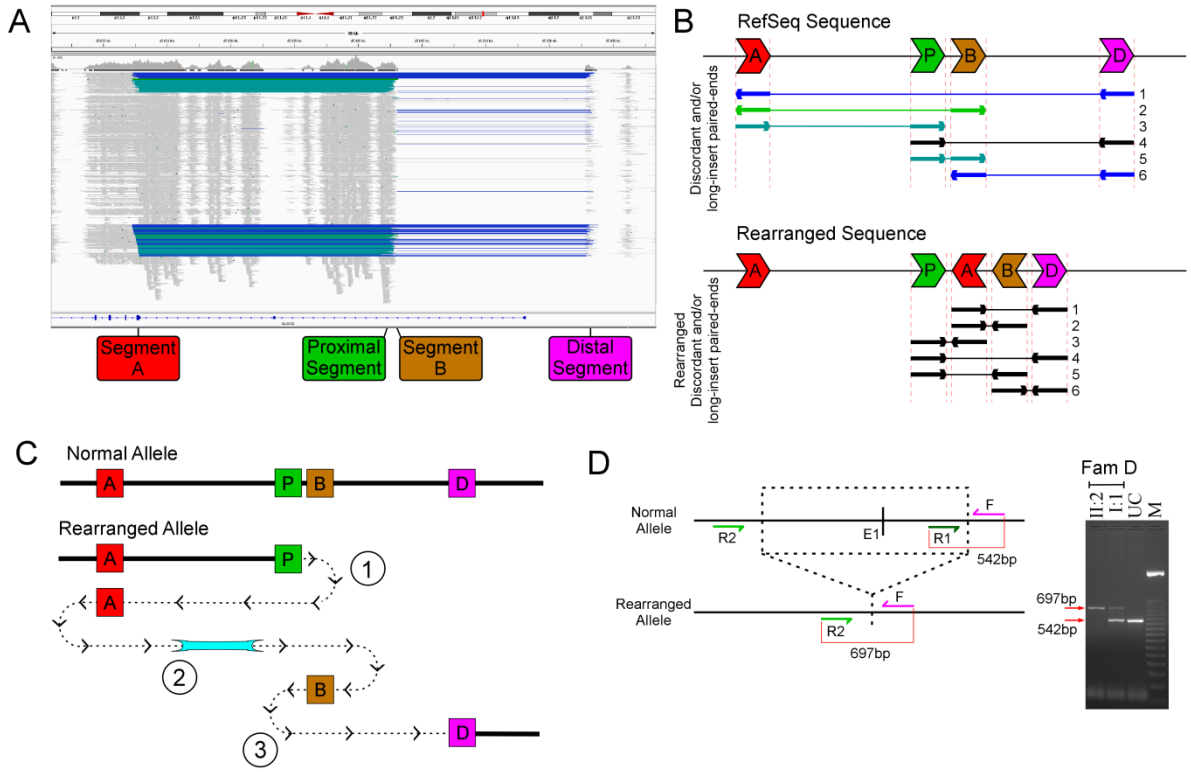

Figure S1. Resolving the Complex Rearrangement

(A) IGV images of the aligned paired-ends obtained via targeted sequencing in affected individual D-II:2. Proximal segment and Distal segment represent sequences in the vicinity of either end of the deletion breakpoints, whereas Segment A and Segment B are the sequences inserted in the complex rearrangement. For interpretation of the colors please refer to the IGV user guide on the IGV website (interpreting color by pair orientation). Briefly; grey paired-ends: both ends are facing each other (normal orientation); blue paired-ends: both ends are in left orientation; aqua paired-ends: both ends are in right orientation; green paired-ends: both ends are in opposite orientation.

Figure S1. Resolving the Complex Rearrangement (continued)

(B) Schematic representation of the paired-ends that are discordant and/or long-insert (>1000 bp) as visualized in IGV. Detailed examination in family D using IGV showed 6 different types of discordant and/or long-insert (>1000 bp) paired-end reads around the deleted sequence, shown in (A). The upper panel shows 6 types of abnormal paired-end reads in the targeted sequencing data. Rearrangement of the genomic sequence, as shown in the lower panel, resolves discordant and/or long-insert paired-ends and predicts the complex rearrangement sequence. A: Segment A; P: Proximal segment; B: Segment B; D: Distal Segment.

(C) Schematic representation of the events that lead to the complex rearrangement. Circled numbers 1, 2, and 3 indicate the joining events during formation of the complex rearrangement, as follows, Event 1: Joining of Proximal segment and inverted Segment A; Event 2: Joining of inverted Segments A and B via a 13 bp joining segment; Event 3: Joining of inverted Segment B and Distal Segment.

(D) The 3-primer PCR designed to detect wild-type and rearranged alleles of *ELMO2*. Schematic representation of the PCR primer binding positions on the genome shows that the wild-type allele produces a 542 bp long PCR product, whereas deletion due to the complex rearrangement produces of a 697 bp long product using a different reverse primer (shown on the left). The right panel shows the agarose gel electrophoresis of the PCR products for affected individual D-II:2, who is homozygous, and her father (D-I:1), who is heterozygous for the complex rearrangement. An unrelated control (UC) is homozygous for the wild-type allele. M: 100bp DNA ladder (Promega).

>out_236 size=4247 cov=147.71
Proximal Segment
(45.027.684) GGAGGCACAGAGGAGTTAAGTAGAAGGCTCAGTGTCACATAGCTAGCAAGTGGCACA
GCCAGAATTTGATACCAGGTTGTCTGGTGTTGCTGGAAAGCCATGAGAAAGCAGGTGGCTCTGCACCTGA
CCCGCAGCAGGTGCTTTGTGGAGATTTCTGGTTTGTGTATCTGAAACCAAAGCACACTGAGGCTAAGAAA
CCTTCACAGCAAGAACTCACCATTGTAACAGAAGACAGCTCTCCACTGTCTACAGGTGGGCCACACTCCC
TCGTGTGCTATTTGGTCCTTTACAATCTAGCCATCCTGGACTACGGGCTATTTCTATAAGGCAGGCCATG
TTCTTTCAATTCTTCTGTACCTTTGCACATTCTCTTCCTCCTACTGACTGTCAGAAGAGCTCCTATTCAA
GCATCAGAGCCTAGTTCGGATGTTACCTCCTCCTTGTACTAGTCTTAGCTTTCTCTACTTTCCCTGGCAA
AAGTAAATAGGACAGGGGCCTCTGTGTTCTCACAGCATCCTGTTCATACTTCCGTTAATGAGTACGATTT
TGTCATACTCTATTACAGTTACATATTTACACATCTCCACTAGCTCCTCCTCCAGAACAGGTATAACTCT
GCAGTCTCATAACCTAGCACAGCACTTGGTGTCCAGTGAAGGCTCAGTAAGCACCTGTGTCTGCTTAAAC
CCAATGGCTCTGATTTCTTCCACTCCTGTGAACCAGGCTGGCTCCAAACAGACAGGGACAGGCATGAACT
GTGCAGGCTGTCTGGTGTTCCCTCTGCGTCCCAATACCCTCTAACTACACAGTATTTCCATTGTTTAACA
GTTTGTTTTGGCTGGGCGCAGTGGCTCACACCTGTAATCCCAATGCTTTGGGAGGTCAAGGCAGGAGGAT
CACTTCAGGCCAGGAGTTCGAGACATTTCTCTACAAAAAATAAAAATTAGCTGGGCATGGTGGCGTGTGC
CTGTAGTCCCTAGCTACTCAGGAGGCTGAGGCAGGAGAGTTGCTTGAGCCCAGGAGTTCGAGGCTGCAGT
GAACTATGATCATGTCACTGAACTCTAGCCTGGGTGACAAAGTGAGATCCTGTCTCTATTAAAAAATAAA
AATAAAATAAAAAACTGTTGTTTTCATATCAAACATTAGAATAAGTCTTACTGAAAAATCAGGGTTAGCA
CCCCTAACTCTAGTTGAAAGAAAGAGGAAAACCTCCCTCTGCTTTTCTCCCTATCGAAAAGAAACATCAG
GAGATAGGAGACTAGAAATAATTCTGTTCTCCAGATAATATTCCCAGGATAAAGGATCTCCTTATAGGGA
ACCCTTCCAGCACGTGTTTGCTTACTCCCTTCATTTTCATTCTAGAAAGGAAGTAGAAATTAGGTCAAAG
GAATTCAGTAACATTGCAAAATTCTCAGGGTTATAAATAGCCTCTTGCTCCGCCACTCAGCAGTACTGTA
GCTCAATTGCAAACCACCAGCATAAGGGAGCTGTAGTTCCATATCCAGGCCCAGAGGGCCCCTTCCGGAT
TAAACAACTCCCCACCCTTCTACCTTCCACTCCTCTTTAAGCATTACAGATATAAGGATGATTTGGAAAA
CTCAAAATGCTACAAAACAGGAGACAGGCACACACTGACCTGATGACAATTTTACTATAAGTCATAAGAA
TGAAAGGCCAGTTTTTCAAACACAGAGCTGGGAAAAGTAGAGAAAAATAGGAACATTAGTGTCTCCAATG
GAGCAGTCTCTAAGTGGCTTCTAGAAGGTGTGCTTATAAAATCAGCACTGTTACAGAAGCCCCATGGAGC
TTTATCAATCACCCATGCAGTGACTGCTGCTTCACGGAGCTGGATTCTGAGAGCAGGATTGGAAACCGAA
TCTTAAGGAATGAAGTGAAAGATGATCTCCTCCTATTAGTAAGGAATTTGGGATGAAGAATGCCAGGTTT
CCAGCTCCCCTCCTTCCCCCTATTCCTTTAAGGATAAGAACGGATGTGTACTTTTTGTTCAGTTATTTGG
CTTTTGATTTGGTGAAGGAGGCATGGGTAAGTTTGGTTTATGTTTCCTGCAACAGAATGCAACCTCATCA
AGAAGGCAAGTTGGAGTCACGCCCTTTCTAATCGAGAACACAATCTCTATAAAGGCTTCCCCCTCTGAAA
TCTTCTCATCTGAGAAGTGATTCAACTTCCCTTAGTTCAGTCCACTGAATGACGATCAGACTCTGAGGTA
CAGAAAAGGGAGGATTTGACTGGCAGAGATTAAGGTTCTTATGTTTACTGCTGGAAGCCCTGGGAAGGAC
CACCATACCAACAGCAGCTGAGGTTTCCCCTTTTTGTTGAAGTATGTTAGACACAGGACTCATTCACACA
TGGTAAAAAGCCACAAACTTACATAGAGGCAAAGGTGTGGTGAGAAGGGGTGTGGGGGCAGGGGAACTAT
TTGGGTTTCTTCATCTTGATTCCTGCTGTAAGAATGGCCTGGGTCTTCTCTTATCCTGCACAGACACCTT
CTGTAGTGTTCCTATACTTAAAGAATAGTGCTTAAGTAAGCTCCTTAGCAGAGCATTCAACTTACTCCAG
TTCCACCGTGGCTCTGTGGTGGAACTGGCTTTCAGATTCGCTTTTGCAGATGCCATGTTCTCACCAGACC
ACCTGTTCCCTGAAAAACCATGCTCTTCTGAGTCTGTATGTTTGCTTGTGCTATTATTTCCTCTTCCTTG
TCCAGCTGGCAAACTTCAACTCAACCTTCAAGGCCCAGCTAAGATAATCACTCTTCTATGTGGCTTTCCT
AATCCTCTCACCTCAGGGAAAATTAATTGCAGCCTCATCTGTGATCCCAGTCTTCTGTACATACCTTCCT
GATCCTACTGATTTATAATTCTCTATGTGCAGTCTCTTCCCTGGCTACGATAGGTGTGATGTGCATACCA
GCAGCGGCAGTATCCCTGGGAGCCCAGACCCACCCAATCAGAATCTGCCTTCAAACAAGATCCTGAGGTG
GTTCAAGTGCATGTTCAAGTCTGGGACATAGGCTCTAGATCAGATAAGGTCCGAGAAACAGTGGTTCTCA
ACTCTGGTTGTGCACCATCAACACACACCCCAGGTCATTTATAAACTCTCAGATGCTCAGGGTTGACCCA
CAGCTCCAGGAGAGTTGACAACCTGAGGGCAAGGACTCATGAAGCCTAAGTCTATTCCCCCATCTACTCT
TCCCCCAGTTTGCAGCACACTGCCTGCCACATAGCTGTGTCCACAGAATTCCACAGGAAAATTCCCTCCA
GGGTGCCTCCAGACCTAAATGCCTTCAGAAGAGAGTGAAAACACTACTGACTGAGGATTATTAATTGCCT
AGAACTTTCCAAATCCCTAACCACAATGACTGAAGAGATGAATTTACAAAAAGTCAGTGTTTACAAACCA
CTTACCTCAGTTTTTGGAAATGAGAGGAAACAGAAACTGAGATGGAAAATACAGATGAACTTCAGAATTA
AACTTTAGAAAACCGTGATT(45,031,190)

Segment A inverted
(45,023,171) GCAGCCGTGTCTGTGTTTTTGTCTCGCAGAATTAGAGCCCATTGGGAACGATGCCAC
CACCGTCAGACATTGTCAAAGTGGCCATTGAGTGGCCAGGTGCTAACGCCCAGCTCCTTGAAATCGACCA
GGTATGCTCCTGAAGTGAGAAGCAGTGGTTCAAGGAAAGGCACCTGGGGAGTGCATGGCAGAGGACATCT
TGAGGGATGGGGACCACCGGCATCAAGAGTAAGAACGAGCAACAGGAAGGCTAAGCTTTGGGC
(45,022,912)

Joiningsegment
TTACAACTTAAGC

Segment B inverted
(45,031,259) TTAGTTGTAACCCAGGACTCTTCCCAGCACACCACACTCCCTCCCTACCCAAGCTCC
(45,031,203)

DistalSegment
(45,037,129) CAGTGGGCAACTAGGTTCAGGTGCCGTGTTTTCAGGCTGGAATCAAATAGGAGGAGT
ACCTGCAGCTGAATGTCATGATTACACAAATGCAATTGTGTCTGGCACGTGGGAGAGGATAGTAGAGATT
CTGAGCTTTGTAACCTTGCAGACCTTTGTGCTATTTACCAGCTGTTTGTCCCTGGGTAAGTTACTAGATC
TCTCTGAGCCTGTCTCCTCATGTGTACAATGGGGAGAATAACAGTACCAGCCTTAATGGATTGTTGTGAG
AAATGAGATCACTGTAAATATACAACAGTTAGCAAAATGTCTGCATTTAAGTGCTCAATAAATTGTAAAT
TATAAAATTTTAAAATTATAGTAGGCCTTCCATAAGTACTTATTGTGTGAGTGAATTATCTACCCCTCTC
AGT(45.037.538)

Figure S2. *De novo* Assembly of the Sequence Around Complex Rearrangement

Figure S2. *De novo* Assembly of the Sequence Around Complex Rearrangement (continued)

Presented here is the continuous sequence of the complex rearrangement assembled using paired-end reads from targeted massively parallel sequencing of D-II:2 that align between Chr20:45,027,684 and Chr20:45,037,538 on the reference sequence. The segments of the complex rearrangement are named as shown in Figure 2. The starting and ending positions of each segment on the reference genome are indicated in red for Proximal Segment, Segment A inverted, Segment B inverted, and Distal Segment, whereas no position is indicated for the 13 bp long joining segment sequence that joins inverted Segments A and B. Sequences highlighted in yellow show microhomology segments at breakpoint junctions of Proximal Segment-Segment A inverted and Segment B inverted-Distal Segment. Note that the joining segment is not a random sequence, but consists of 2 microhomology segments near the boundaries of Segments A and B highlighted in blue and green. The sequence highlighted in blue is a direct repetition of 6 nucleotides near the boundary of Segment A inverted with an additional thymidine. The sequence highlighted in green is an inverted repetition of 6 nucleotides near the boundary of Segment B inverted. Presence of >1 microhomologies, several basepairs apart from breakpoints suggests that >1 DNA synthesis and trimming event may have occurred during event 2 (Figure S1C).

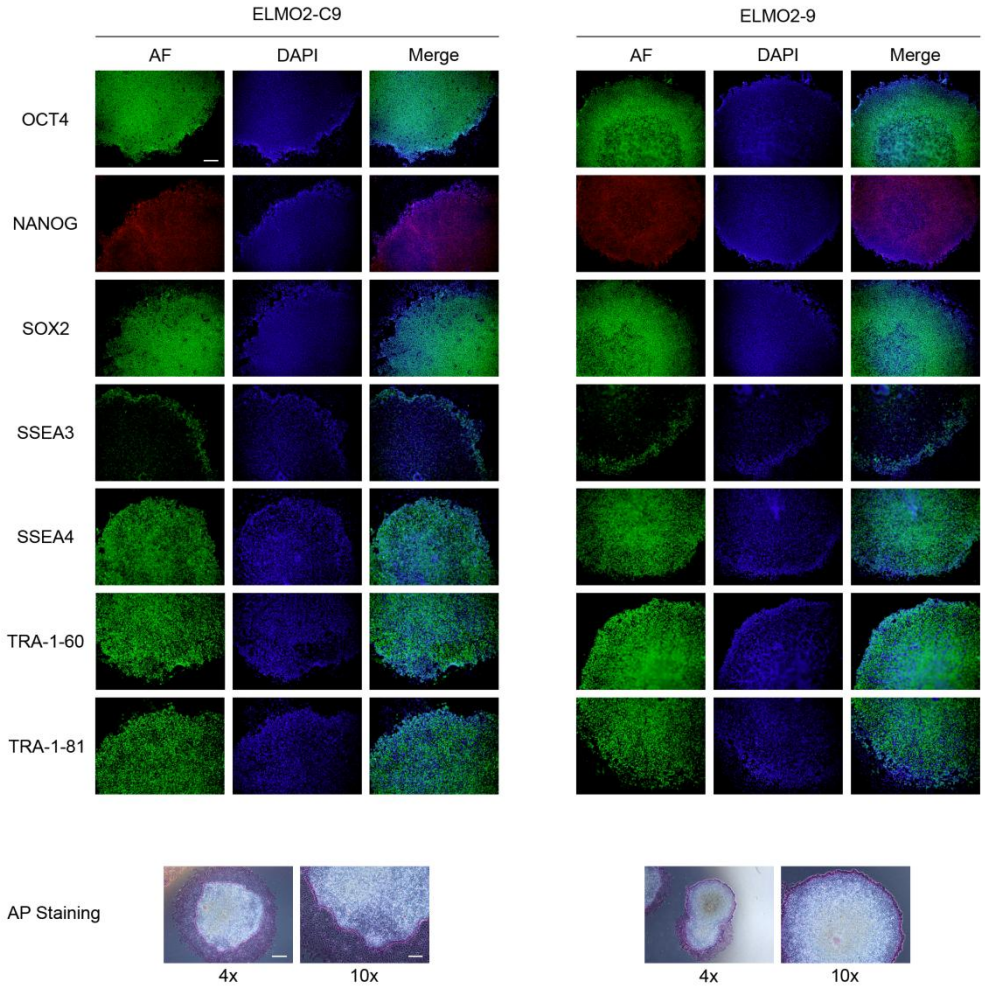

Figure S3. iPSCs Derived from Human Dermal Fibroblasts Are Pluripotent

Immunofluorescence (IF) images of control (ELMO2-C9) and affected individual (ELMO2-9) iPSCs stained for various markers of pluripotency, along with alkaline phosphatase (AP) staining. Scale bars on IF and AP staining at 10× magnification represent 200 µm. Scale bar on AP staining at 4× represents 500 µm. AF: Alexa Fluor; DAPI: 4',6-diamidino-2-phenylindole. To generate human iPSCs, retroviral vectors encoding the human cDNAs of KLF4, SOX2, OCT4, and C-MYC (Addgene) were used and cells were grown in KnockOut DMEM containing 20% KnockOut serum replacement, 2 mM L-glutamine, 1% NEAA, 0.1 mM beta-mercaptoethanol, 1% NEAA, 0.1% penicillin and streptomycin, and 4 ng/ml bFGF on irradiated fibroblast feeders. iPSC colonies were manually picked after 3–4 weeks and subsequently adapted to Matrigel-coated (Corning) dishes.

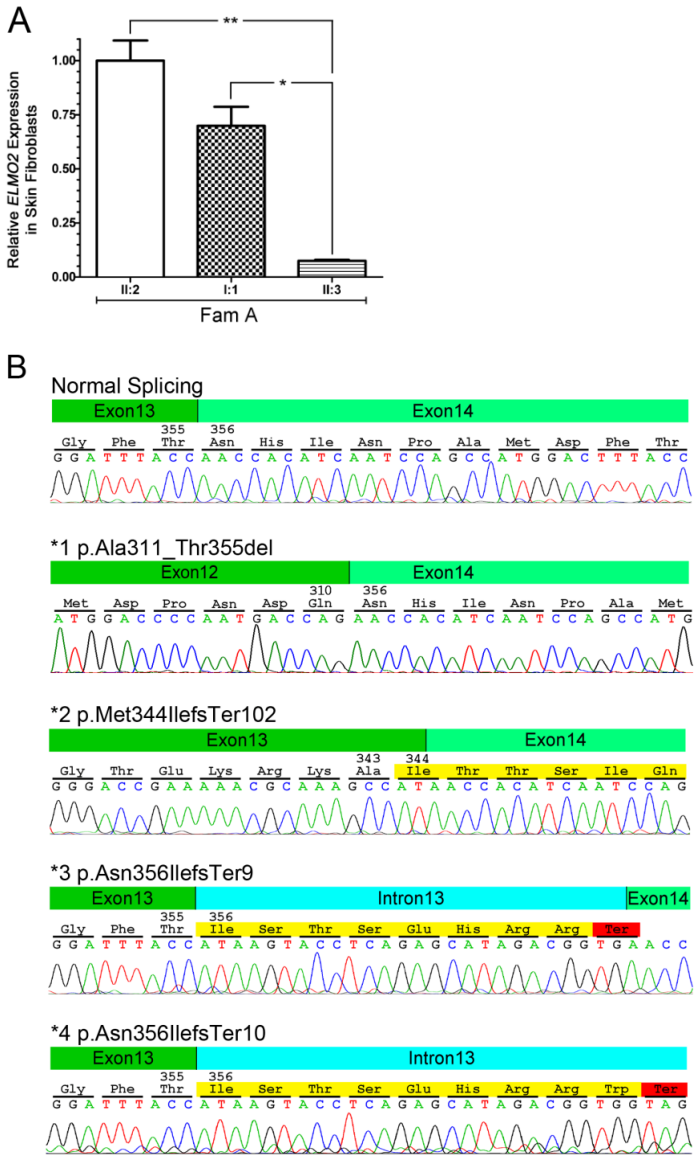

Figure S4. The Effect of the c.1065+1G>A Mutation in *ELMO2* on the RNA Level

(A) Expression of *ELMO2* detected via qRT-PCR in the non-carrier sibling control (A-II:2), the heterozygous father (A-I:1), and the affected individual (A-II:3), respectively. Briefly, total RNA for qRT-PCR was isolated from primary fibroblasts grown to 70% confluence using TRI Reagent (Sigma-Aldrich). cDNA was generated via reverse transcription using a QuantiTect Reverse Transcription Kit (QIAGEN). Quantitative real-time PCR (qRT-PCR) was performed using Jump Start SYBR Green Mix (Sigma-Aldrich) and the housekeeping gene *ACTB* to normalize gene expression. Data are shown as mean ± SEM, unpaired two-tailed t-test. *p<0.05; **p<0.01. **(B)** Sanger sequences with amino acid annotations of the 4 aberrantly-spliced transcripts in affected individual A-II:3, as compared to the canonical splice variant.

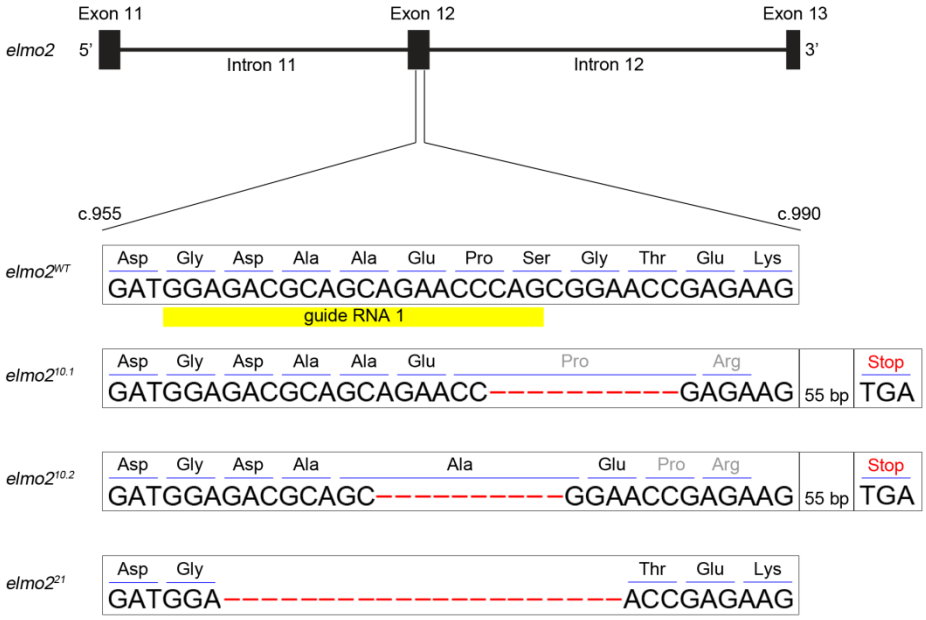

Figure S5. Generation of Zebrafish *ELMO2* Allelic Series

Schematic diagram showing nucleotide deletions on zebrafish genomic loci in the 3 *elmo2* knockout alleles, along with amino acid annotations. Yellow box represents guide RNA 1 target loci.

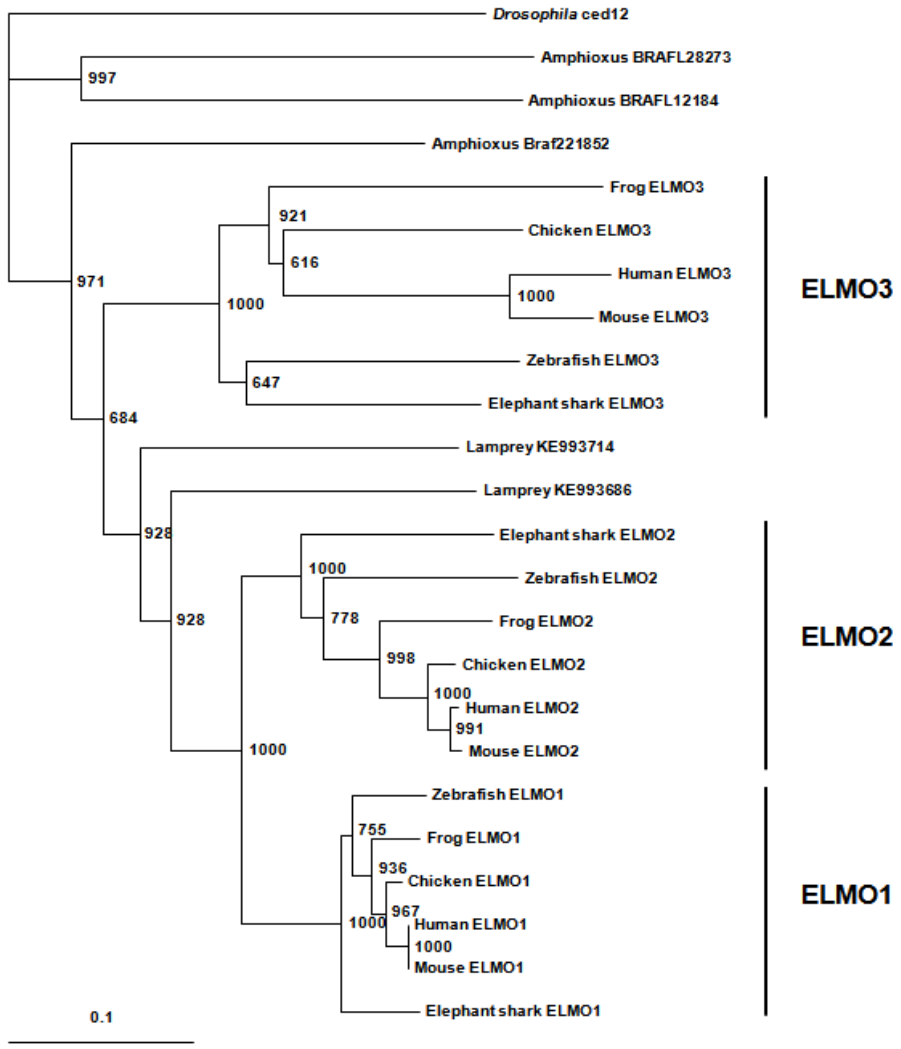

Figure S6. Phylogenetic Analysis of ELMO Protein Family

A molecular phylogenetic tree showing the relationships between vertebrate and amphioxus ELMO proteins based on neighbour-joining analysis. Phylogenetic analysis of the ELMO family was performed using the NCBI reference sequences of ELMO1, ELMO2, and ELMO3 proteins of the following species: human (*Homo sapiens*; GenBank: NP_055615, NP_573403, NP_078988), mouse (*Mus musculus*; GenBank: NP_525027, NP_525026, NP_766348), chicken (*Gallus gallus*; GenBank: NP_001026165, XP_417479, NP_001243730), frog (*Xenopus tropicalis*; GenBank: XP_002939462, NP_001008123, XP_002931693), zebrafish (*Danio rerio*; GenBank: NP_998256, NP_001186987, XP_009296233), and elephant shark (*Callorhinchus milii*; GenBank: XP_007887897, XP_007883848, XP_007904034).

Figure S6. Phylogenetic Analysis of ELMO Protein Family (continued)

To identify the orthologous proteins of amphioxus and lampreys, the genome sequence databases of amphioxus (*Branchiostoma floridae*, JGI Genome Portal) and Japanese lamprey (*Lethenteron japonicum*, Japanese Lamprey Genome Project) were searched using BLASTP and TBLASTN. The single *Drosophila melanogaster* ced-12 protein (GenBank: NP_609548) was used as an outgroup for phylogenetic analysis.

The ELMO protein or deduced amino acid sequences from the these species were aligned using ClustalX2. The sequences were then manually trimmed of all sites that were not unambiguously aligned. Phylogenetic analysis of amino acid sequences was performed using the neighbor-joining method implemented in ClustalX2, with outputs displayed using TreeView (Figure S6). Branch lengths are proportional to evolutionary distance corrected for multiple substitutions; the scale bar denotes 0.1 underlying amino acid substitutions per site. Figures on branches indicate robustness of each node, estimated from 1000 bootstrap replicates. Three ELMO proteins of jawed-vertebrates (ELMO1, ELMO2, ELMO3) form a monophyletic group generated by the two gene duplication events at the origin of vertebrates: one that gave rise to the Elmo3 and Elmo1/2 paralogous groups, and a second that gave rise to the Elmo1 and Elmo2 paralogous groups around the time of appearance of "jaw" and dermal bones in vertebrates.

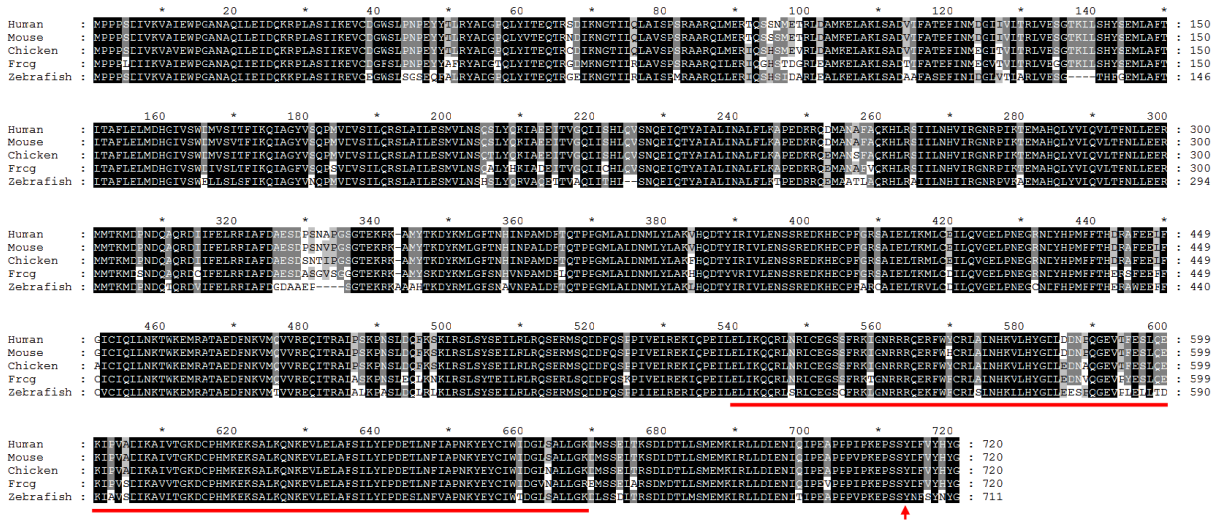

Figure S7. Comparison of ELMO2 Proteins in Vertebrate Model Species

Amino acid sequences from human (*Homo sapiens*, NP_573403), mouse (*Mus musculus*,NP_525026), chicken (*Gallus gallus*, XP_417479), frog (*Xenopus tropicalis*, NP_001008123) and zebrafish (*Danio rerio*, NP_001186987) were aligned by ClustalX2. Black shades denote 100% conserved regions (including similarity groups); dark and light grey shades represent 80% and 60% conserved regions respectively. Critical domains interacting with other molecules such as the PH domain (cd13359, red underlines) with DOCK and Tyr-713 with Axl (red arrow) are highly conserved amongst different species .

Supplemental Tables

Filtering / Individuals	Fam A	Fam B	Fam C	Fam D
	II:4	II:3	II:5	II:2
Mean coverage	303	332	339	149
Percentage of chr20:43,655,782-46,924,866 region with ≥4 coverage	99%	99%	99%	98%
Total number of variants in region chr20:43,655,782-46,924,866	5125	5009	5041	5196
≥4 coverage and ≥15 genotype score	4646	4413	4632	4392
Not found or GMAF and ESPMAF <0.01 in dbSNP138	2357	2065	2281	2019
Not found in in-house database (n=279)	2185	1903	2133	1884
Homozygous variants	269	275	286	265
Missense, Stop Gain/Loss, Splice site, insertion, deletion, indel variants	1 (*ELMO2*)	5 (*ZNF335*, *NCOA5*, *ELMO2*, *NCOA3***, *SULF2*)	1 (*ELMO2*)	2 (*OCSTAMP*, *NCOA3***)
Common genes with variants	**1 (c.1065+1G>A in *ELMO2*)**		**1 (c.1802-1G>C in *ELMO2*)**	**Deletion of 1st exon of *ELMO2****

Table S1. Filtering and Prioritization Scheme for Targeted Sequencing

Mean coverage of exons and percentage of exons covered ≥4 times in the critical interval are shown for each individual. Variants from targeted sequencing for each individual were filtered for variants that had low quality, low coverage, and high frequency in the general population (1000 Genomes, Exome Sequencing Project, and IGBAM in-house exome database). Subsequently, potentially deleterious single nucleotide or small deletion/insertion variants (missense, stop gain/loss, splice site, insertion, deletion, and indel variants) that are homozygous were listed for each individual. Variants in *ELMO2* were common in affected individuals from Families A, B, and C; however, a complex rearrangement involving the first exon of *ELMO2* that was missed by variant calling was detected in Family D, indicated by *. The 9 bp in-frame deletion in *NCOA3* is indicated by **, which is homozygous in 10 of 498 additional individuals without vascular malformation in the IGBAM in-house database. GMAF: Global minor allele frequency, taken from the 1000 Genome Project; ESPMAF: Exome Sequencing Project minor allele frequency.

Filtering / Individuals	Fam A					Fam B				Fam C				
	I:1	I:2	II:2	II:3	II:4	I:1	I:2	II:3	II:4	I:2	II:1	II:2	II:3	II:5
Mean coverage	17	40	43	25	24	23	32	24	19	3.6	2.9	15	19	27
Percentage of exons with ≥4 coverage	80%	91%	94%	88%	87%	87%	90%	88%	86%	32%	24%	86%	85%	88%
Total number of variants	170546	214233	269255	199825	198015	196031	222757	200628	189187	99529	109633	193365	189967	224412
≥4 coverage and ≥15 genotype score	115913	157273	189878	140626	148795	135869	156292	139228	125610	39013	29279	121989	131678	164804
Not found or GMAF and ESPMAF <0.01 in dbSNP138	38133	39215	49253	35707	35733	34007	39810	36885	31746	14978	10061	31738	38639	41859
Not found in in-house database (n=279)	34608	34619	43178	31518	31772	30112	35063	32551	28041	13819	9210	28215	33900	37078
Heterozygous in parents, homozygous in affected children and different from affected children in unaffected children	68					254				5				
Missense, Stop Gain/Loss, Splice site, insertion, deletion, indel variants	5					10				1				
In target region (chr20: 43.6-46.9 Mbp)	1 (*ELMO2*)					3 (*ZNF335*, *NCOA5*, *ELMO2*)				1 (*ELMO2*)				
Common in three families	**1 (c.1065+1G>A in *ELMO2*)**									**1 (c.1802-1G>C in *ELMO2*)**				

Table S2. Filtering and Prioritization Scheme for Exome Sequencing

Mean coverage of the exome and percentage of exons covered ≥4 times are shown for each individual. Variants from exome sequencing for each individual were filtered for variants that had low quality, low coverage, and high frequency in the general population (1000 Genomes, Exome Sequencing Project, and IGBAM in-house exome database). Subsequently, potentially deleterious single nucleotide or small deletion/insertion variants (missense, stop gain/loss, splice site, insertion, deletion, and indel variants) that are consistent with Mendelian inheritance for autosomal recessive disorders and located in the critical region delineated by homozygosity mapping were listed for each individual. Variants in *ELMO2* were common in affected individuals from Families A, B, and C. GMAF: Global Minor Allele Frequency, taken from the 1000 Genome Project; ESPMAF: Exome Sequencing Project minor allele frequency.

Primers	Forward (5'->3')	Reverse (5'->3')
DNA Sequencing		
Human		
ELMO2 Ex13–In13	AGCCAAGCCCATTTCTGTC	ACCATCAACAAAGCAAAGCA
ELMO2 In19–Ex20	ATTGTGAAGGAGAGGGGAAG	TCAGGAATAGAGAGGGGAAGA
ELMO2 Ex22	TGAGCCCCATCAGAAAAGA	AAAAGACAAGGCACCAGAATG
ELMO2 Ex1	GCAGGTACTCCTCCTATTTGATTC	R1: AATCCCTAACCACAATGACTGA R2: ACTCACTTCATACTCTTATGTGAAAGC
ELMO2 In12 – In13	GTTAGCCGATTCACCTGCTG	CTACCCACTCTAGCTGACCG
Zebrafish		
elmo2 genotyping	TGTCCGCTCATGTTCAACAC	GTGTGCACTGACGCTGAATC
cDNA Sequencing		
ELMO2	GAAGAAAGGATGATGACCAAGA	GCAGGATTTCACAGAGCA
RT-PCR		
ELMO2 Splice	CTGAAGGCTCCTGAGGACAA	TTGTCTTCCCGGCTACTGTT
Quantitative Real Time PCR		
Human		
ACTB	CGCAAAGACCTGTACGCCAAC	GAGCCGCCGATCCACACG
ELMO2.1	CAGACTCGCAGTGACATTAA	GCCATCCATGTTGATGAACT
ELMO2.2	GACCTTAAACTTCATCGCACCT	AGGTCACTCTTGGTCAGCTC
ELMO1	TGCCAACTGAACTTCATCGC	TCATGTCCTTCCCGAGTAGC
ELMO3	CGGACATGATCTTTGCCAGG	CCTAGGTCGTCCCCATCTTC
GAPDH	TGAACCAAGTGCTTAGC	CGCATGGACTGTGGTCATGAG
Zebrafish		
elmo1	AAACAGCAGCGTCTCAATCG	CCAGAACTTGTCCTGTCTCCT
elmo2	GCGTTCTCCATCCTCTACGA	AGATCCTTCCCTAGCAGAGC
elmo3	TAAGGAGGTGCTGGACTTGG	TTCTGGACGAGGCGATGAAA
actin	GATCTTCACTCCCCTTGTTCA	GGCAGCGATTTCCTCATC
Cloning		
ELMO2 ORF pCS2+ BamHI_XbaI	GTAggattcATGCCACCACCGTCAGACAT	ACTCGtctagaGCTCAGCCATAGTGATAGACAA

Table S3. List of Primers

All primer sequences used for DNA and cDNA sequencing, RT-PCR, and cloning, for both humans and zebrafish.